

Yu.M. Vaskovskyi, A.M. Melnyk, O.I. Tytko

ELECTROMAGNETIC VIBRATION DISTURBING FORCES AT THE ECCENTRICITY OF ROTOR OF TURBOGENERATOR

Electromagnetic vibration disturbing forces in different variants of the rotor displacement from an axis of the stator bore is carried out. Investigation for TG type TGV-200-2 by finite element method in COMSOL Multiphysics is carried out. The field mathematical model of static and dynamic eccentricity is described. The amplitude vibration disturbing forces are greatest, when a static eccentricity direction coincides with an axis of the stator winding phase is shown. The diagnostic features static and dynamic eccentricities are formulated. The most value of forces in the point with minimal air gap is shown. The diagnostic features static and dynamic eccentricities and the method of diagnostic eccentricity are formulated. Diagnostic feature of static eccentricity is to change the amplitude Maxwell stress tensor is established. The dynamic eccentricity diagnostic features are appearance in the spectrum of vibration disturbing forces rotating and multiple harmonics. References 8, tables 3, figures 6,

Key words: turbogenerator, field mathematical model, electromagnetic vibration disturbing forces, Maxwell stress tensor, eccentricity, damage of rotor, diagnostic feature.

В статье исследовано электромагнитные вибровозмущающие силы турбогенератора при наличии дефекта ротора. Исследования выполнены для турбогенератора типа ТГВ-200-2 методом конечных элементов в программном обеспечении COMSOL Multiphysics. Описано полевую математическую модель статического и динамического эксцентриситета, которая позволяет смоделировать сигналы датчика вибраций как функции реального времени. Выполнено серию расчетов электромагнитных сил при различных вариантах смещения ротора с оси расточки статора. Показано, что при возникновении эксцентриситета наблюдается существенное увеличение вибровозмущающих сил и наибольшее значение сил будет в точке с минимальным воздушным промежутком. Введено новые диагностические параметры и предложено методику диагностирования эксцентриситета. На основе проведенного математического моделирования установлено, что диагностическим признаком статического эксцентриситета является изменение амплитуды тензора магнитного тяжения, а признаком динамического эксцентриситета – наличие в спектре вибровозмущающих сил оборотной и кратных ей гармоник. Библи. 8, табл. 3, рис. 6

Ключевые слова: турбогенератор, полевая математическая модель, электромагнитные вибровозмущающие силы, тензор магнитного тяжения, эксцентриситет, дефект ротора, диагностический признак.

Introduction. Recently the problem of timely monitoring and diagnostics and eliminate injuries powerful electric machines is particularly important due to the aging fleet of existing machines and the increasing number of cases of an emergency stop with significant economic losses. In particular this applies powerful synchronous turbogenerators (TG), which are widely used in thermal and nuclear power plants. Particular attention is paid to TG rotor which is complex and node design.

In recent years in Ukraine and abroad, studies of the physical processes that occur in the presence of synchronous generator rotor their defects [1-8]. By defects rotor may also include uneven of air gap (AG) between the stator and rotor (eccentricity). This failure can occur as a result of manufacturing defects, and in the operation of TG. When the rotor eccentricity refers displacement axis rotor stator bore axis [4]. There are: a) static eccentricity (SE) in which the AG configuration for rotation of the rotor remains unchanged, i.e. the minimum and maximum period do not change their position; b) dynamic eccentricity (DE), in which the minimum and maximum of AG rotates with the rotation of the rotor.

TG rotor eccentricity appearance leads to a distortion of the magnetic field in AG, the occurrence of electromagnetic forces sided magnetic attraction, of additional higher harmonics of the field, increase local overheating. In the array of rotor turbine flow eddy currents that lead to significant heat damage and structural elements of the rotor (grooving wedges bandage rings).

The eccentricity of the rotor may be the installation of the rotor TG or during its operation (as a result of wear

of bearings, offset supports, flex shaft, etc.). Significant identify the nature and magnitude of the eccentricity of the rotor in the synchronous generator without the withdrawal of the mode of operation is a relevant and complex engineering task of solving the effectiveness of which depends on the amount of electricity generated, durability, efficiency and safety of TG.

There are many methods for detecting and diagnosing damage of electric machines, the main ones are the methods of mechanical, vibration, electromagnetic diagnostic method for the analysis phase current range and others [1-3, 6]. The feasibility of selecting one of these methods for diagnosing rotor eccentricity of the TG due to their reliability and sensitivity of diagnostic parameters, the complexity of technical implementation, the cost of hardware and methodological support and other factors. The comparative analysis of these methods has shown that the solution SE and DE of the TG appropriate to use the method of vibration diagnosis, due to the simplicity of implementation and high reliability of the identification of defects. To determine the diagnostic features is necessary to study electromagnetic forces that change the appearance of the SE or DE.

The goal of the work is to study methods of mathematical modeling of electromagnetic vibration disturbing forces under static and dynamic eccentricity of the TG and to determine diagnostic features for diagnosing these types of defect. The modeling is performed using the finite element method implemented in a software environment *COMSOL Multiphysics*. Diagnosis is sug-

gested to conduct on the basis of spectral analysis of functions of tensor magnetic stress tensor using fast Fourier transform (FFT).

Problem definition. Mathematical model involves solving equations of the electromagnetic field in the core of the TG and definition vibration disturbing forces in the selected stator point where conventional vibration sensor is placed. Given the considerable axial length of the core of the TG compared to the long pole graduations, just consider the field in two-dimensional approach in cross section. We shall consider quasi-static processes, suggesting that all field functions change in time for the harmonic law. In general, the basic equations of the electromagnetic field is relatively complex amplitude of the magnetic vector potential, which has only one spatial (axial) component \vec{A}_z , in the stator coordinate system is as follows:

$$\vec{A}_z - j\omega\mu\gamma\vec{A}_z + \mu\gamma\omega_R(R \times \text{rot}\vec{A}_z) = -\mu\vec{J}_{ext}, \quad (1)$$

where \vec{J}_{ext} is the density of external currents (in our case, this is the density of current in the stator slots, which is set to correspond to the stator windings circuit); ω is the angular frequency of changes over time of the magnetic vector potential; ω_R is the angular frequency of the rotor rotation; γ is the electrical conductivity; R is the radius-vector of an arbitrary point of the rotor. The angular frequency changes over time magnetic potential and angular rotor speed depends on the choice of coordinate, which implemented the solution. For synchronous machines without eddy currents in the stator and rotor cores equation (1) takes the following form:

$$\Delta\vec{A}_z = -\mu\vec{J}_{ext}. \quad (2)$$

Field sources are external currents densities of three phases of the stator winding:

$$\begin{aligned} \vec{J}_{Aext} &= I_m u_n / S_n, \\ \vec{J}_{Bext} &= I_m u_n [\cos(-2\pi/3) - j\sin(-2\pi/3)] / S_n, \\ \vec{J}_{Cext} &= I_m u_n [\cos(-4\pi/3) - j\sin(-4\pi/3)] / S_n, \end{aligned} \quad (3)$$

where I_m is the amplitude of the current in the phase of the stator winding; u_n is the number of series-connected conductors in the stator slot; S_n is the sectional area of the stator slot.

Equation (2) is complemented by homogeneous boundary conditions of the first kind in the line of the outer surface of the stator yoke which limits the calculated area:

$$\vec{A}_z|_G = 0. \quad (4)$$

The value of μ at each point calculation area where the ferromagnetic materials present is determined by the corresponding magnetization curves. The components of magnetic induction in the Cartesian coordinate system defined by relations:

$$\vec{B}_x = \partial\vec{A}_z / \partial y, \quad \vec{B}_y = \partial\vec{A}_z / \partial x, \quad (5)$$

Vibration disturbing forces density is proportional to the magnetic stress tensor that has the physical dimension of the pressure (N/m²). Modules of normal and tangential components of magnetic stress tensor are expressed as:

$$T_n = \left| \frac{1}{2\mu} (\vec{B}_n^2 - \vec{B}_\tau^2) \right|, \quad T_\tau = \left| \frac{1}{\mu} (\vec{B}_n^2 \cdot \vec{B}_\tau^2) \right|, \quad (6)$$

respectively normal (directed along the vector normal to the surface at a given point) and tangential (directed along the tangent to the surface at a given point) projection of magnetic induction. Normal and tangential components of the magnetic induction determined through induction projection vector in Cartesian coordinates by the expression:

$$\begin{aligned} \vec{B}_n &= \vec{B}_y \cos\alpha + \vec{B}_x \sin\alpha = (y\vec{B}_y + x\vec{B}_x) / R_\delta, \\ \vec{B}_\tau &= \vec{B}_x \cos\alpha - \vec{B}_y \sin\alpha = (y\vec{B}_x - x\vec{B}_y) / R_\delta, \end{aligned} \quad (7)$$

where x, y are the projections of the radius-vector on the axis of the coordinate system; R_δ is the radius of the bore of the stator. Further deals radial vibration occurring by the action of the normal component of the magnetic stress tensor.

To take into account changes over time of the tensor model involves changing the configuration time calculation area while moving the rotor relative to the stator. Moving of the rotor are simulated by changes of coordinates x, y of points of the rotor. Changes $\Delta x, \Delta y$ of rotor coordinates by a time Δt are given by the following formulas:

$$\begin{cases} \Delta x = \cos[\omega_R \cdot (t + \Delta t)] \cdot x - \sin[\omega_R \cdot (t + \Delta t)] \cdot y - x; \\ \Delta y = \sin[\omega_R \cdot (t + \Delta t)] \cdot x + \cos[\omega_R \cdot (t + \Delta t)] \cdot y - y. \end{cases} \quad (8)$$

The time interval T on which analyzed signal analysis is carried out corresponds to one period is one complete revolution of the rotor – for bipolar TG $T = (0 \dots 0.02)$ s. Number of calculation steps is 200, meaning that one time step is 10^{-4} s. During one step back rotor relative to the stator a third of the rotor division that meets the conditions of accuracy.

A model of static and dynamic eccentricity. Relative value of the eccentricity is determined by the formula:

$$\varepsilon = \frac{\delta_{\max} - \delta_{\min}}{\delta_{\max} + \delta_{\min}}, \quad (9)$$

where $\delta_{\max}, \delta_{\min}$ are the maximal and minimal values of AG, respectively. In this paper the static and dynamic rotor eccentricity are considered at shifting its axis relative to the axis of the stator bore by two coordinates X (horizontal eccentricity) and Y (vertical).

To simulate the eccentricity using the above-mentioned field mathematical model that takes into account the rotation of the rotor at the time. Fig. 1 shows the displacement of the rotor axis stator static (*a*) and dynamic (*b*) eccentricity. In this model, SE simulated displacement axis of the rotor relative to the stator geometrical axis by the amount ΔR which generally is decomposed into bias coordinates of the center of the rotor on the Y axis on the value of $\Delta Y = \Delta R \cdot \sin\alpha$ (Fig. 1,*a*), and the displacement coordinates on the X axis equals $\Delta X = \Delta R \cdot \cos\alpha$.

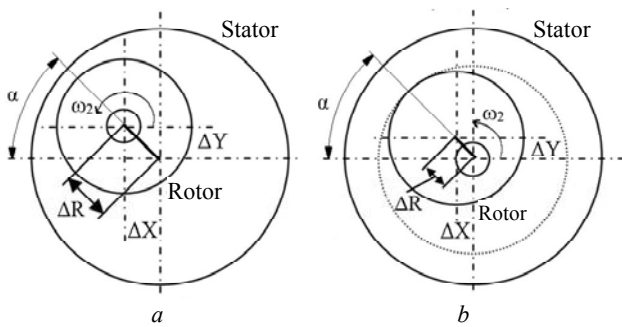


Fig. 1. Models of static (a) and dynamic (b) eccentricity

Calculated area includes two sub-areas: fixed, which includes a stator and a moving containing a rotor. The border between the two subregions is in the middle of AG, and with uneven refers to sub-areas of the stator. DE is modeled by geometric displacement of axis of the rotor relative to the axis of rotation on the value ΔR . This move all points of the rotating subregion by the coordinates X and Y are the same and the equation of motion will match the expression (8). Note that at DE to the calculated rotating subregion rotor not only, but also uneven AG are included.

Mathematical model (1-8) can simulate the signals of conventional vibration sensors (vibration acceleration sensors) as a function of time. To this end, points 1, 2, 3 of conventional location of sensors (Fig. 2) by the expression (7) is calculated normal component of magnetic stress tensor (MST) as the value of the acceleration is proportional to value of the magnetic disturbing force.

Results of investigations. Investigations are conducted by the example of the TG type TGV-200-2. Based on the above described mathematical model further investigated magnetic disturbing forces arising due to normal component tensor magnetic tension (ceteris paribus technical condition of the stator). As you know, one sensor setting is not sufficient to determine whether the SE because of vibration investigated crowns on teeth in the stator bore three points 1, 2, 3. Fig. 2 shows a picture of the distribution of the magnetic vector potential and magnetic flux density at time $t = 0.02$ s in the active zone of the TG.

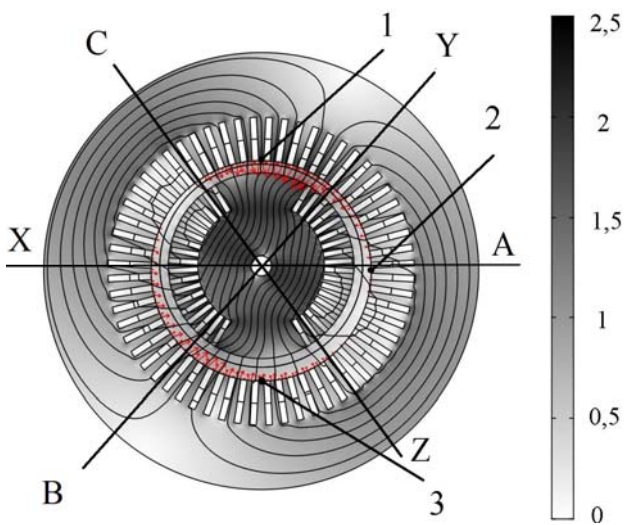


Fig. 2. Distribution of the magnetic vector potential and magnetic flux density with calculated points

Modeling was performed for nominal operation mode of the generator with good condition (no SE and DE) and when defective (presence of eccentricity). SE was simulated by displacement of the rotor along Y coordinates with the angle $\alpha = 90^\circ$. Fig. 3 and Fig. 4, respectively, in these three points on the crowns of teeth of the stator depicted settlement functions of the magnetic stress tensor over time in the presence of SE and DE (for $\varepsilon = 0.25$ when the rotor displacement along the axis of symmetry phase A). Figures shows that the signals of the 1st and 2nd sensors shifted between a time phase that meets their spatial shift of 90° along the stator bore. The numbers on the charts correspond to the designation of calculated points.

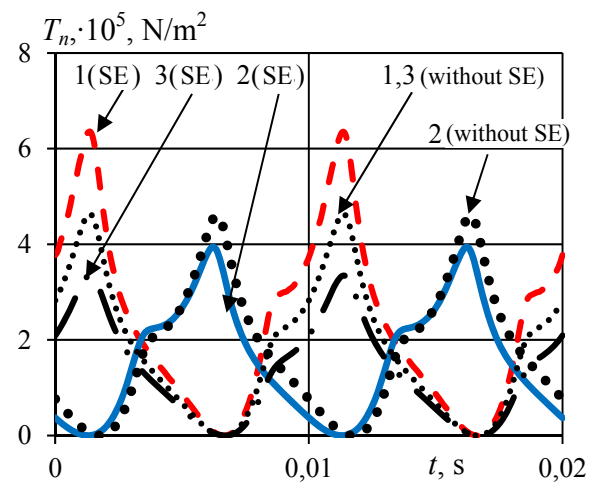


Fig. 3. MST functions at calculated points at presence of SE

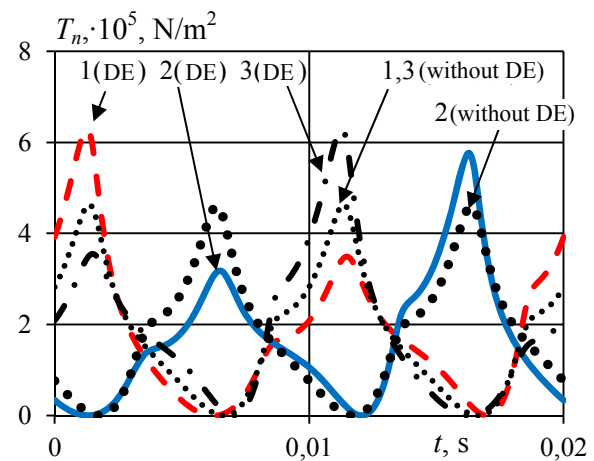


Fig. 4. MST functions at calculated points at presence of DE

From the results of spectral analysis for different values of SE ($\varepsilon=0.1$, $\varepsilon=0.2$ and $\varepsilon=0.25$) we can see increasing amplitude harmonic 100 Hz respectively of 10, 15 and 30%. Comparison of MST when SE shows that when $\Delta R = 25$ mm ($\varepsilon=0.25$) in point 3 of the largest AG amplitude of MST decreased 1.4 times and at point 1 –increased 1.37 times. This effect is clearly seen from the graphs at the DE when the rotor rotates value of AG is constantly changing, and MST function is asymmetric and obviously that will have additional spectrum harmonic multiples rotating frequency.

In view of the above, an effective method of analysis of the time functions of electromagnetic vibration disturbing forces is determination of their spectral composition using fast Fourier transform. Fig. 5 shows the amplitude of MST at SE depending on the value of ε for different variants displacement of the rotor relative to the stator winding phase zones. Note that different variants of displacement of the rotor axis of rotation were conducted at a fixed position axis phase zone A which coincides with the modeling of a horizontal axis. MST amplitudes are shown in three points of location of sensors (points 1-3). The results of mathematical modeling showed that if SE when $\Delta R = 25$ mm ($\varepsilon=0.25$) amplitude of the fundamental harmonic electromagnetic forces increased by 32 %. Also present spectrum vibration disturbing forces components that create vibrations at frequencies of 200, 300, 400 Hz are respectively 15, 18 and 12 % relative to the fundamental harmonic.

Thus, the most dangerous is eccentricity when the eccentricity direction coincides with the axis of the stator phase. So, Fig. 5,a shows that even at $\varepsilon = 0.1$ amplitude of vibration disturbing forces increases by 13 %.

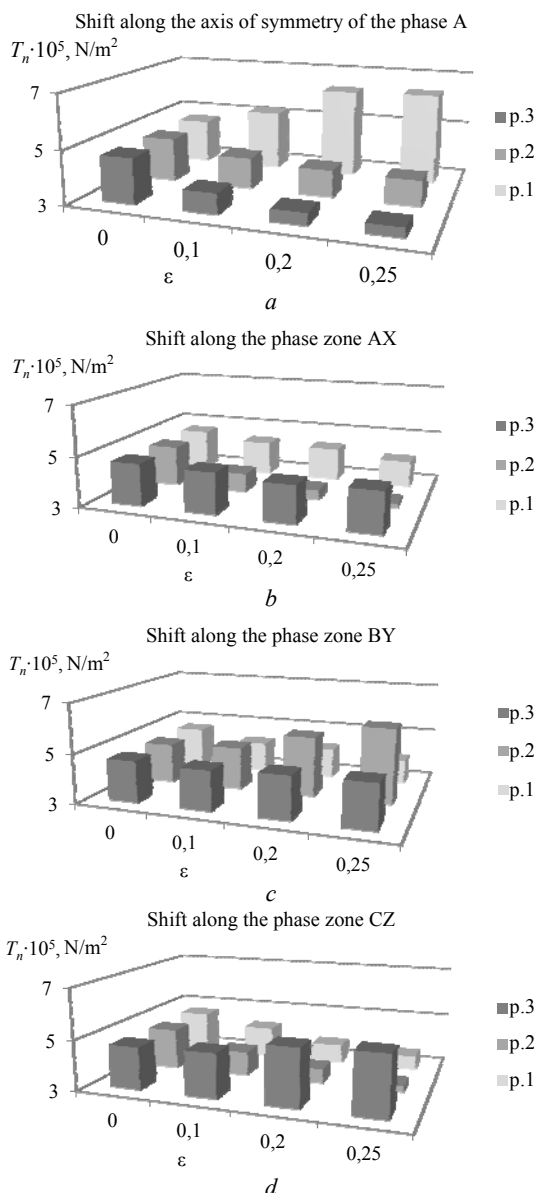


Fig. 5. Amplitudes of magnetic stress tensor vs eccentricity factor

Figure 6 for the DE case shows amplitude spectra of MST for 50 Hz (a), 150 Hz (b) and 250 Hz (c).

From Fig. 6,a,b one can see that the amplitude of each harmonic of the rotation frequency of 50 Hz and aliquot to it 150 Hz are 12 % (at $\varepsilon=0.1$), 25 % (at $\varepsilon=0.2$) and 30 % (at $\varepsilon=0.25$) of the basic harmonic 100 Hz. These results can be the basis for the formulation of appropriate diagnostic features and determining the presence of a defect.

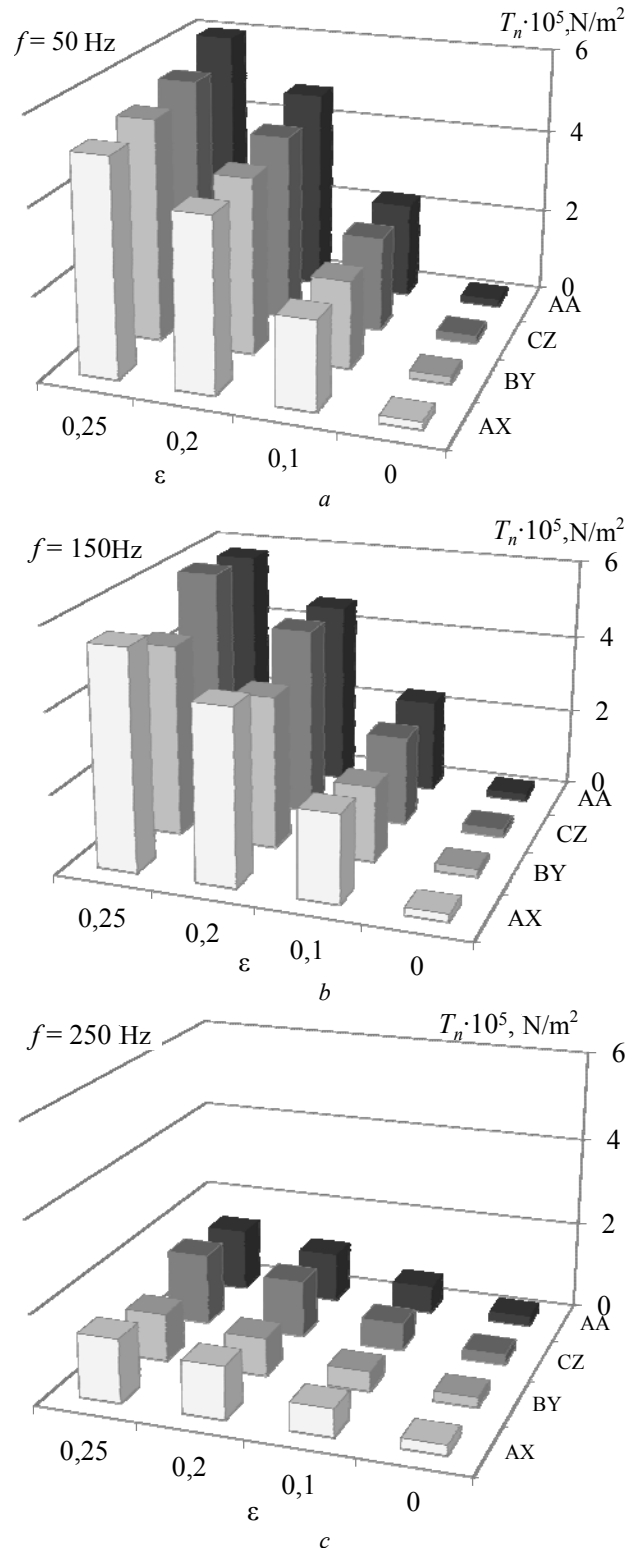


Fig. 6. Amplitudes of magnetic stress tensor spectrum frequencies vs value of eccentricity

Important technical assessment of the state of the generator with the appearance of damage provides analysis of changes in total harmonic vibration of all, characterized by RMS. Change factor of RMS of the MST spectrum k_{rms_T} describes ratio of RMS of the MST spectrum of the damaged TG to RMS of the MST spectrum of the un hurt TG and is calculated as follows:

$$k_{rms_T} = \sqrt{\frac{\sum_{i=1}^N |T_{i_fault}|^2}{\sum_{i=1}^N |T_{i_no_fault}|^2}}, \quad (10)$$

where N is number of accounted harmonics in spectrum; i is the number of harmonics; T_{i_fault} , $T_{i_no_fault}$ are the amplitudes of the i -th harmonics of MST in spectra of vibration sensor signal regarding damaged and un hurt TG.

Table 1 shows the range of RMS of MST spectrum calculated in point 1. Legends AX, BY and CZ correspond to the rotor displacement along the axis of the corresponding phase zone, marking AA meets at the location of the sensor in the area at minimum AG at the rotor displacement along the axis of symmetry of the phase A of the stator winding. Table 1 shows that the overall level of vibrations of electromagnetic origin at the SE is the largest when the direction of eccentricity coincides with the axis of the stator winding phase (in this case with a vertical axis). Electromagnetic vibrations under other phases at SE (AX, BY, CZ) decrease.

Table 1

Ration of the RMS change of MST spectrum at eccentricity

	E	AA	AX	BY	CZ
SE	0.1	1.111	0.912	0.904	0.93
	0.2	1.326	0.954	0.899	0.838
	0.25	1.329	0.967	0.851	0.8
DE	0.1	1.015	1.012	1.01	1.01
	0.2	1.079	1.038	1.02	1.074
	0.25	1.123	1.065	1.035	1.112

Therefore, to determine the maximum vibration sensor must be installed opposite phase stator winding axis. When installing the wrong sensor measurement results will indicate the reduction of vibrations that will not re-

veal the presence of SE. At DE total level of vibration is independent of the direction of eccentricity. However, despite the fact that the vibrations of electromagnetic origin is less than the SE, you need to take into account the fact that there are vibrations of mechanical origin associated with fluctuations in the center of mass of the rotor. Therefore, the total vibrations can be more than the vibrations at the SE.

Generalize the results of mathematical modeling by introducing diagnostic parameters at different values of AG and direction of displacement of the rotor relative to the stator winding phase zones. Table 2 shows the diagnostic feature k_{δ} which allows to diagnose the occurrence of SE based on measurement of the amplitudes of sensor signals.

$$k_{\delta} = T_{fault} / T_{no_fault}. \quad (11)$$

Table 3 shows the value of diagnostic feature k_e characterizing the ratio of the difference of the amplitudes of MST in the first and second points (k_{e12}) and the first and third points (k_{e13}) according to the amplitude of NTM in the first point at different values of the coefficient of eccentricity.

$$k_{e12} = \frac{T_{\tau1} - T_{\tau12}}{T_{\tau1}}; \quad k_{e13} = \frac{T_{\tau1} - T_{\tau13}}{T_{\tau1}}. \quad (12)$$

The obtained diagnostic parameters are given in Table 2 and 3. The results allow to formulate a reasonable method of diagnosing eccentricity. To determine the SE we must mount at least two sensors, for example, the top and bottom of the vertical axis, as the most likely direction of displacement of the rotor along the vertical axis. A comparison of the signals of two sensors will help diagnose the occurrence of eccentricity. To diagnose DE it is enough to mount one sensor vibration because with this type of defect of AG at one point is not permanent. After measuring the sensor signal is decomposed in Fourier series and if there are harmonics of the signal multiple rotating frequency, it can be argued the presence of DE.

Table 2

Diagnostic feature k_{δ}

Phase zone of the stator winding relatively that the rotor displacement was modeled	AG between stator and rotor, δ , mm						
	75	80	90	100	110	120	125
AA	1.371	1.356	1.126	1	0.802	0.74	0.716
AX	0.873	0.933	0.94	1	0.992	0.958	0.982
BY	0.857	0.906	0.911	1	0.984	1.01	1.021
CZ	0.764	0.806	0.91	1	1.016	1.125	1.145

Table 3

Diagnostic features k_{e12} and k_{e13}

Phase zone of the stator winding relatively that the rotor displacement was modeled	k_{e12}	k_{e13}	k_{e12}	k_{e13}	k_{e12}	k_{e13}
	$\varepsilon=0.1$		$\varepsilon=0.2$		$\varepsilon=0.25$	
AA	0.207	0.281	0.365	0.452	0.379	0.473
AX	0.140	-0.065	0.219	-0.037	0.215	-0.136
BY	-0.119	-0.091	-0.291	-0.125	-0.516	-0.202
CZ	0.063	-0.128	0.045	-0.410	0.084	-0.514

Conclusions.

1. In the event of static eccentricity in the zone of minimum air gap a significant increase of vibration disturbing forces is observed, whose analysis can diagnose damage to the rotor. It is shown that the coincidence of

the direction of the static eccentricity of the geometrical axis of one of the phases of the stator winding, increased vibration is maximized. This fact is expedient to consider when phase stator winding arrangement relative to the horizontal axis turbine generators in the manufacturing

process, taking into account the most likely direction of occurrence of static eccentricity caused, for example, gravity, and so on.

2. In the event of dynamic vibrations of electromagnetic origin eccentricity is less than the static eccentricity, but the mechanical vibration component associated with fluctuations in the center of mass of the rotor, makes a significant contribution to the overall level of vibration. Diagnostic features k_{δ} , k_{e12} , k_{e13} are introduced on which can be built a system and method of diagnosing eccentricity.

3. A diagnostic feature of static eccentricity is changing of amplitude of vibration disturbing forces in the zone of minimum air gap. The spectrum of harmonic of 100 Hz at static eccentricity within $\varepsilon=0.1$; 0.2 and 0.25 in the zone of minimum air gap increases respectively by 10, 15 and 30 %. Diagnostic features of dynamic eccentricity are the appearance in the spectrum of vibration disturbing forces of rotating and multiple harmonics.

REFERENCES

1. Vaskovskyi Yu.M., Tytko O.I., Melnyk A.M. Diagnosis of damage to the excitation winding powerful turbogenerator based on the analysis of electromagnetic forces. *Works of the Institute of Electrodynamics of the National Academy of Sciences of Ukraine*, 2013, no.36, pp. 40-46. (Ukr).
2. Vaskovskyi Yu.M., Tsyvinskyi S.S., Tytko O.I. Electromagnetic processes in the damper winding of hydro generator with eccentricity of air gap. *Tekhnichna elektrodynamika*, 2015, no.1, pp. 65-71. (Ukr).
3. Haidenko Yu.A., Vishnevskiy T.S. Electromagnetic method of diagnostic of static eccentricity of synchronous generator. *Hydropower Ukraine*, 2011, no.2, pp. 52-57. (Rus).

How to cite this article:

Vaskovskyi Yu.M., A Melnyk.M., Tytko O.I. Electromagnetic vibration disturbing forces at the eccentricity of rotor of turbogenerator. *Electrical engineering & electromechanics*, 2016, no.4, pp. 16-21. doi: 10.20998/2074-272X.2016.4.02.

4. Levytskyi A.S., Fedorenko H.M. Characterization of air gap fault in hydrogenerators to data by sensors located on stator. *Hydropower Ukraine*, 2008, no.1, pp. 30-33. (Ukr).
5. Kuchynskiy K.A. Analysis of temperature field of rotor of turbogenerator capacity 300 mW at asymmetry of cooling of grooving zone. *Tekhnichna elektrodynamika*, 2013, no.4, pp. 59-66. (Rus).
6. Milykh V.I., Polyakova N.V Comparative analysis of the variable magnetic field on the surface of the rotor of turbogenerators with different numbers of stator teeth in the load condition. *Tekhnichna elektrodynamika*, 2014, no.2, pp. 29-36. (Rus).
7. Sedky M.M. Diagnosis of static, dynamic and mixed eccentricity in line start permanent magnet synchronous motor by using FEM. *International journal of electrical, robotics, electronics and communications engineering*, 2014, vol.8, no.1, pp. 29-34.
8. Yonggang Li, Guowei Zhou, Shuting Wan, Heming Li. Analysis of unbalanced magnetic pull on turbo-generator rotor under air-gap eccentric fault and rotor short circuit fault. *International journal of advancements in computing technology*, 2013, vol.5, no.4, pp. 523-530. doi: 10.4156/ijact.vol5.issue4.62.

Received 16.03.2016

Yu.M. Vaskovskyi¹, Doctor of Technical Science, Professor,
A.M. Melnyk², Postgraduate Student,
O.I. Tytko², Corresponding member of NAS of Ukraine, Professor,
¹National Technical University of Ukraine
«Kyiv Polytechnic Institute»,
37, Prospect Peremohy, Kyiv-56, 03056, Ukraine.
e-mail: vun157@gmail.com
²The Institute of Electrodynamics of NAS of Ukraine,
56, Prospekt Peremogy, Kiev-57, 03680, Ukraine.
e-mail: ied10@ukr.net